



Supplement of

Changes in apparent temperature and $PM_{2.5}$ around the Beijing–Tianjin megalopolis under greenhouse gas and stratospheric aerosol intervention scenarios

Jun Wang et al.

Correspondence to: John C. Moore (john.moore.bnu@gmail.com) and Liyun Zhao (zhaoliyun@bnu.edu.cn)

The copyright of individual parts of the supplement might differ from the article licence.

Table S1. Apparent temperature thresholds and its health impact (National Weather Service Weather Forecast Office, <https://www.weather.gov/ama/heatindex>).

US NWS Classification	AP threshold	Effect on the body
Caution	27-32°C	Prolonged exposure and/or physical activity can cause fatigue
Extreme caution	32-39°C	Prolonged exposure and/or physical activity can lead to heatstroke, heat cramps, or heat exhaustion
Danger	39-51°C	Heat cramps or heat exhaustion may occur, and prolonged exposure and/or physical activity may cause heatstroke
Extreme danger	>51°C	Very likely to suffer from heat stroke

Table S2. The changes in annual mean precipitation (mm/year) between G4/RCP4.5/RCP8.5 during 2060s and references during 2010s over the domain. Bold indicates that differences are significant.

	G4-2010s	RCP4.5-2010s	RCP8.5-2010s
MIROC-ESM	73.1	50.5	51.8
MIROC-ESM-CHEM	-4.9	43.2	47.1
HadGEM2-ES	69.1	114.1	147.6
BNU-ESM	-41.6	-26.6	6.4
Ensemble	24.0	45.3	63.2

Table S3. Difference of PM_{2.5} concentration between different scenarios for the Beijing-Tianjin province as defined in Fig. 1b during 2060-2069. The PM_{2.5} emission scenarios used in each climate scenarios are in parentheses. Bold indicates the differences or changes are significant at the 5% significant level according to the Wilcoxon signed rank test. (Units: $\mu\text{g}/\text{m}^3$)

Model	G4 (mitigation) -2010s (reference)		G4 (mitigation) -G4 (baseline)		G4 (mitigation) -RCP4.5(mitigation)		G4 (mitigation) -RCP8.5(mitigation)	
	WRF	ISIMIP	WRF	ISIMIP	WRF	ISIMIP	WRF	ISIMIP
MIROC-ESM	-6.4	-7.6	-5.3	-5.2	0.5	0.7	2.2	2.2
MIROC-ESM- CHEM	-7.1	-8.6	-6.0	-6.5	0.5	-0.2	1.9	0.6
HadGEM2-ES	-5.4	-8.4	-4.4	-8.4	1.4	1.3	2.6	2.5
BNU-ESM	-2.9	-5.9	-1.8	-5.3	0.8	1.1	2.5	2.3
Ensemble	-5.4	-7.6	-4.4	-6.3	0.8	0.7	2.3	1.9

Table S4. RRs of the 5 mortality endpoints under G4 with and without considering aerosol deposition from the G4 SAI specification in both PM_{2.5} aerosol “baseline” and “mitigation” scenarios.

G4			population-weighted RR				
			COPD	IHD	LC	LRI	Stroke
“baseline”	No deposition	ISIMIP	1.3167	1.3710	1.4505	1.8063	2.0161
		WRF	1.2968	1.3490	1.4299	1.7844	1.9858
	deposition	ISIMIP	1.3167	1.3711	1.4506	1.8064	2.0162
		WRF	1.2969	1.3491	1.4299	1.7846	1.9858
“mitigation”	No deposition	ISIMIP	1.2958	1.3588	1.4174	1.7313	1.9682
		WRF	1.2820	1.3407	1.4066	1.7323	1.9552
	deposition	ISIMIP	1.2958	1.3588	1.4176	1.7316	1.9683
		WRF	1.2821	1.3407	1.4066	1.7324	1.9552

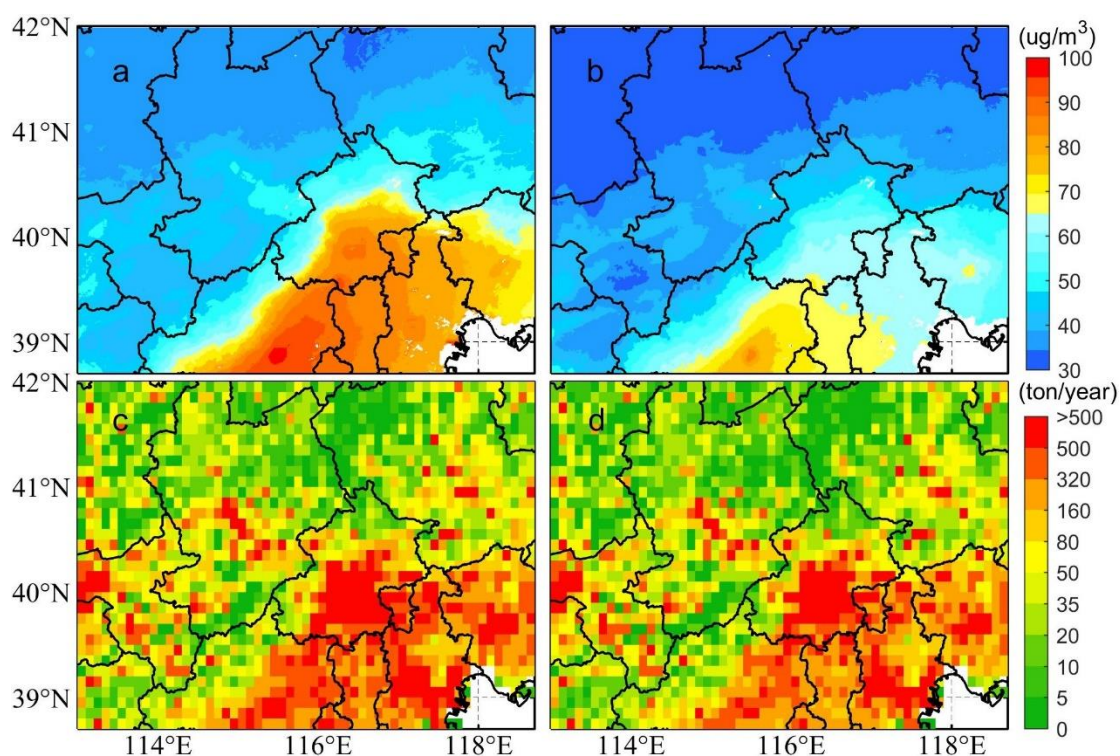


Figure S1. Annual mean PM_{2.5} concentration (a, b) and PM_{2.5} emissions (c, d) map for Beijing and surrounding areas during 2008 (a, c) and 2017 (b, d).

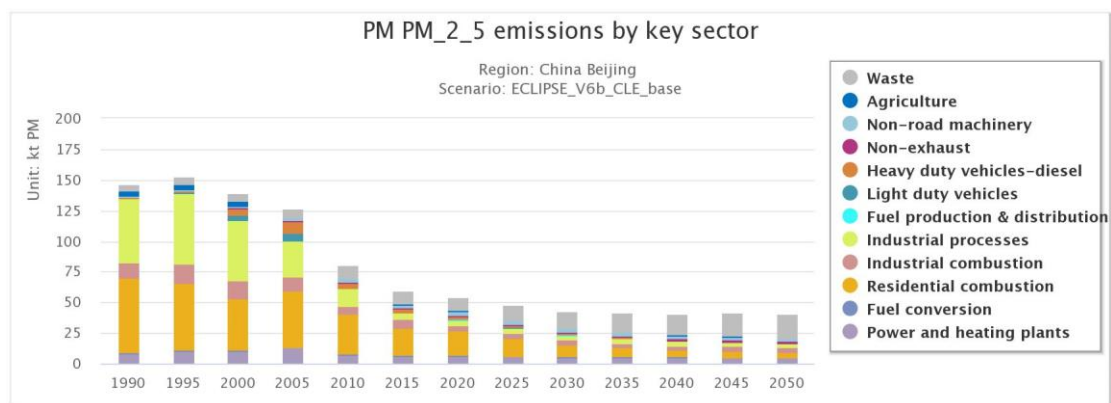


Figure S2. Annual PM_{2.5} emissions from different sources in Beijing under the ECLIPSE V6b baseline scenario (Source: GAINS East Asia online (*tiasa.ac.at*)).

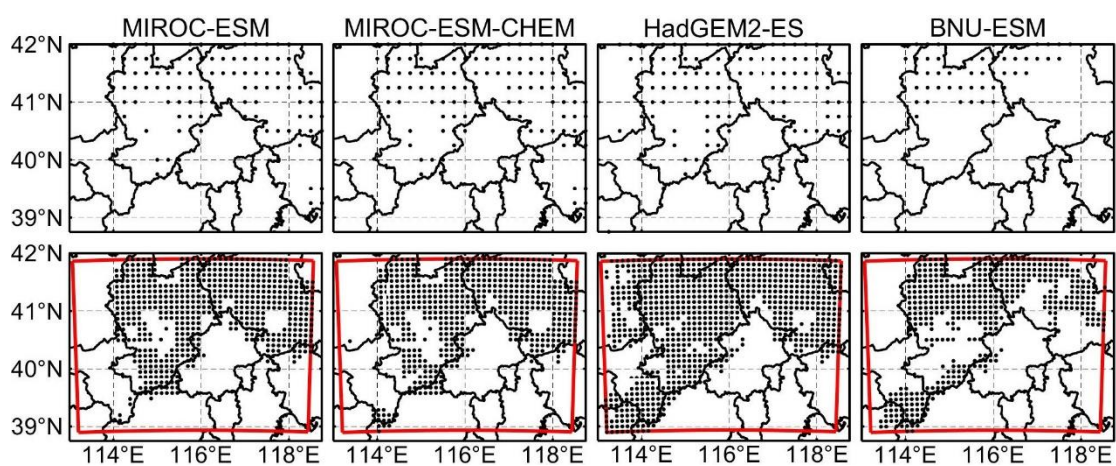


Figure S3. Variance inflation factor (VIF) test of excessive collinearity in our MLR model. VIF > 10 means there is collinearity problem between variables (dotted regions).

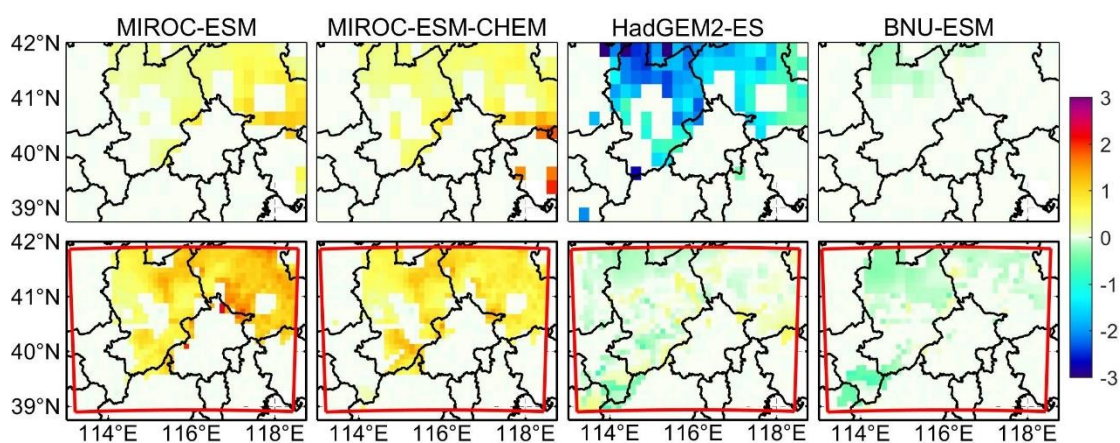


Figure S4. Difference in PM_{2.5} concentration under G4 with “baseline” scenario in 2060s between removing factors with VIF greater than 10 and the full variables model.

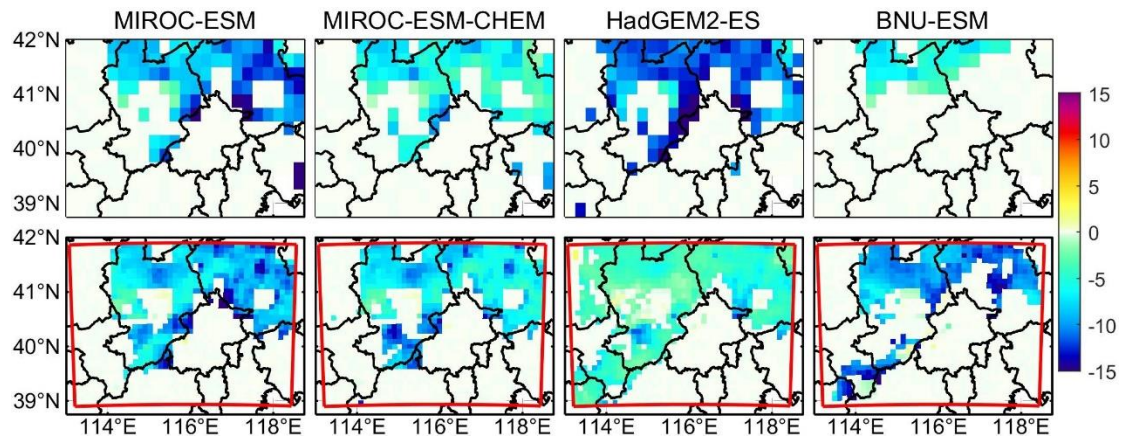


Figure S5. Difference in $PM_{2.5}$ concentration under G4 with “mitigation” scenario in 2060s between removing factors with VIF greater than 10 and the full variables model.

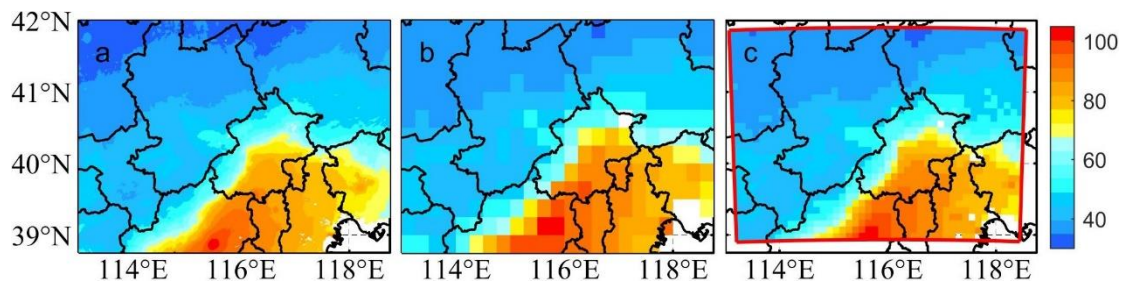


Figure S6. Distribution of observed $PM_{2.5}$ concentration ($\mu g/m^3$) from ChinaHigh $PM_{2.5}$ (a) and ensemble-mean $PM_{2.5}$ concentration from MLR under ISIMIP (b) and WRF (c) results for Beijing and surrounding areas during 2008-2017.

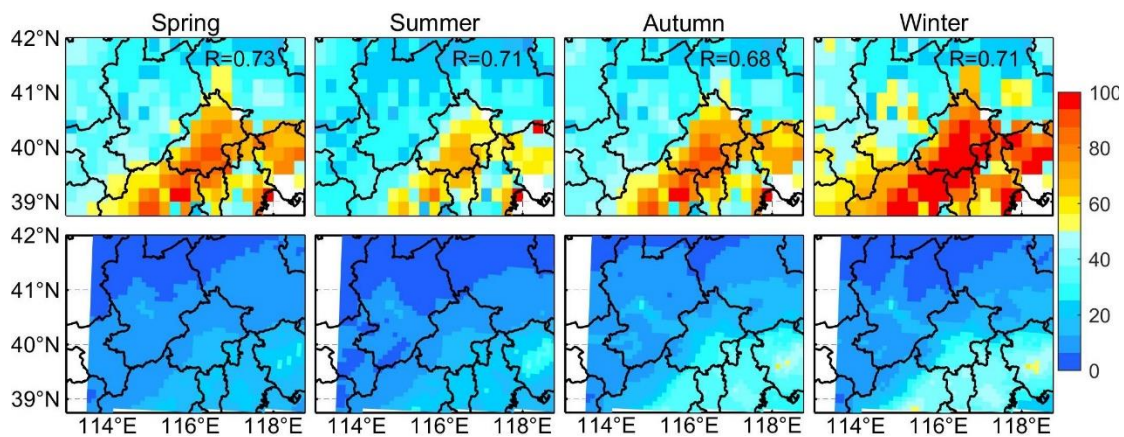


Figure S7. Comparison of our MLR model projection and Li et al. (2023) RCP4.5 simulations. Li et al (2023) use the CMAQ model coupled WRF driven by GFDL-ESM2G and SMOKE model to explore the influence of emissions on air quality in the Beijing-Tianjin-Hebei region of China in 2050. The authors used the dynamical downscaled meteorological factors by WRF driven by GFDL-ESM2G and two air pollution emission scenarios, one is “base” based on the Beijing City Master Plan (2016-2035) and another is “EIT1” based on the emission reduction for WHO Interim Target-1 to compare the impact of different emission scenarios on $PM_{2.5}$ concentration in 2050 under RCP4.5. To assess the performance of our regression model we also downloaded the meteorological variables from GFDL-ESM2G under RCP4.5 and the “EIT1” emission data. The statistical

downscaled meteorological factors during 2008-2017 and 2050 under RCP4.5 were used as independent variables in the regression model to project PM_{2.5} concentration in 2050 under RCP4.5 with the “EIT1” scenario. The top row are calculated by our regression model, and the bottom row are from Li et al. R is the correlation coefficient of PM_{2.5} concentration spatial pattern between our results and Li et al.

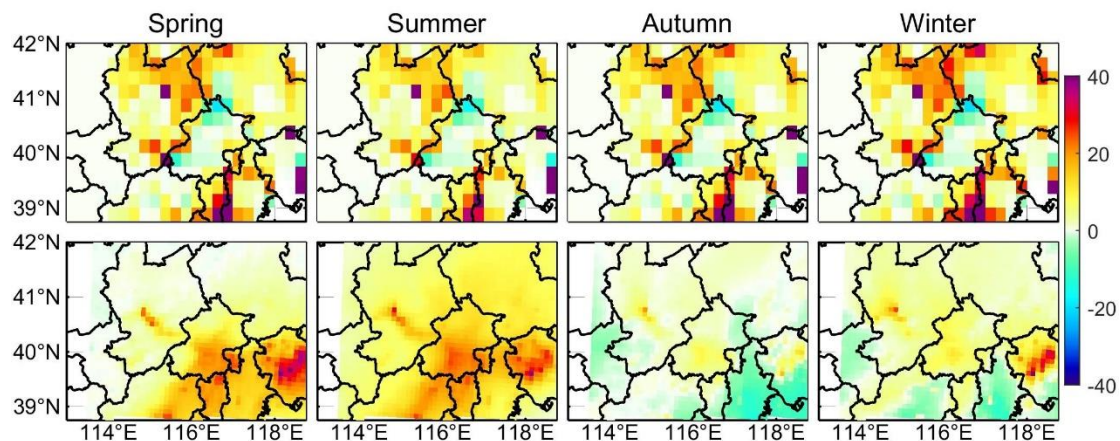


Figure S8. Spatial pattern of differences in PM_{2.5} concentration under RCP4.5 between “base” and “EIT1” emission scenarios in Li et al (2023). The top row are calculated by our regression model, and the bottom row are from Li et al.

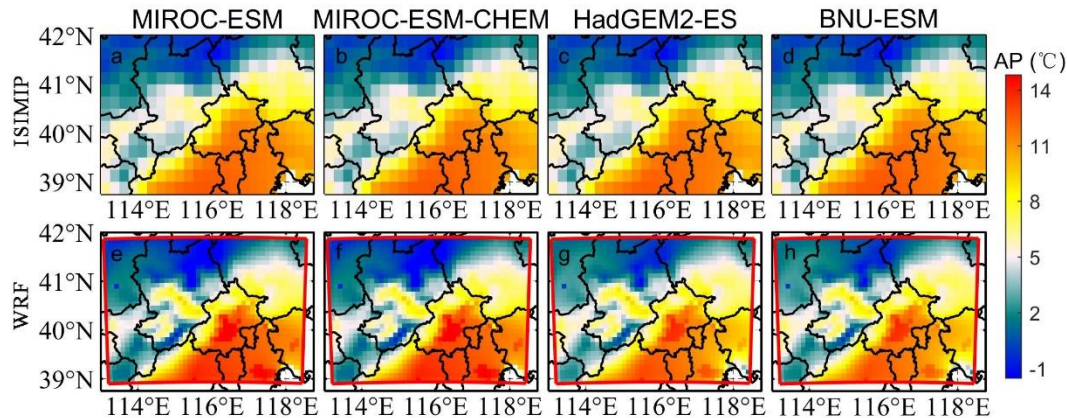


Figure S9. The spatial distribution of mean apparent temperature of MIROC-ESM (a, e), MIROC-ESM-CHEM (b, f), HadGEM2-ES (c, g) and BNU-ESM (d, h) during 2008-2017. The first row are results from ISIMIP method, and the second row are results from WRF.

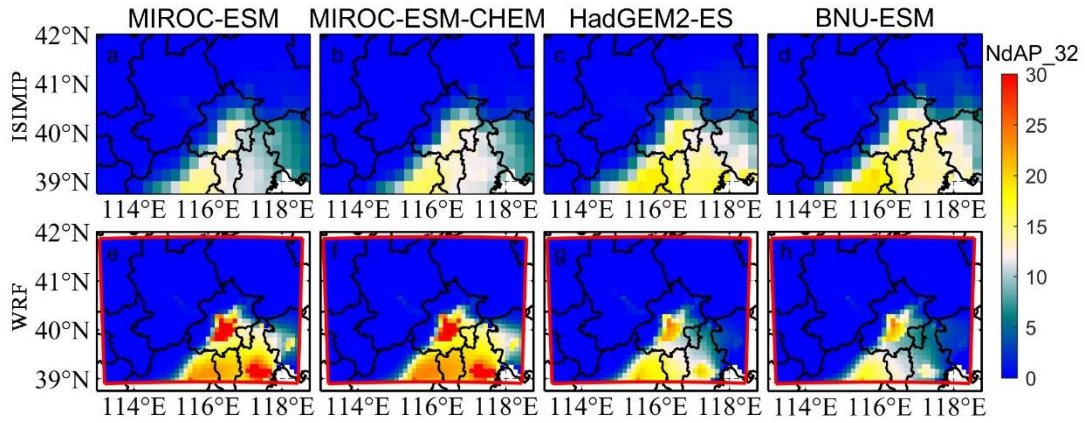


Figure S10. Same as Fig. S9 but for annual mean NdAP₃₂.

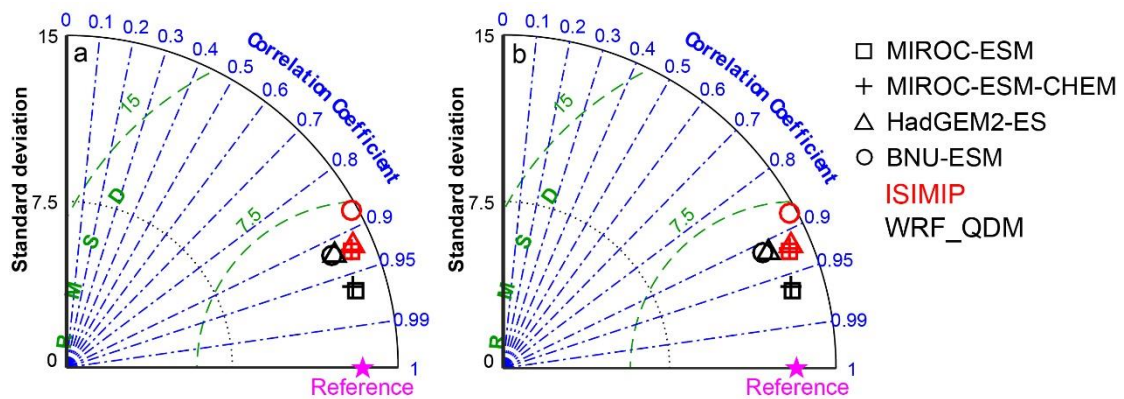


Figure S11. Taylor diagram for daily apparent temperature of four ESMs using two downscaling methods, i.e., ISIMIP (red) and WRF (black) compared to observed data in Beijing-Tianjin provinces (a) and Beijing-Tianjin urban areas (b). The skill of downscaling methods is reflected by the distance from each symbol to the point labelled “Reference”, the CN05.1 reanalysis data. The blue lines are correlation coefficient which represents the similarity between each downscaling data and reanalysis data. The green contours are root mean standard deviation (RMSD), and black contours are standard deviation.

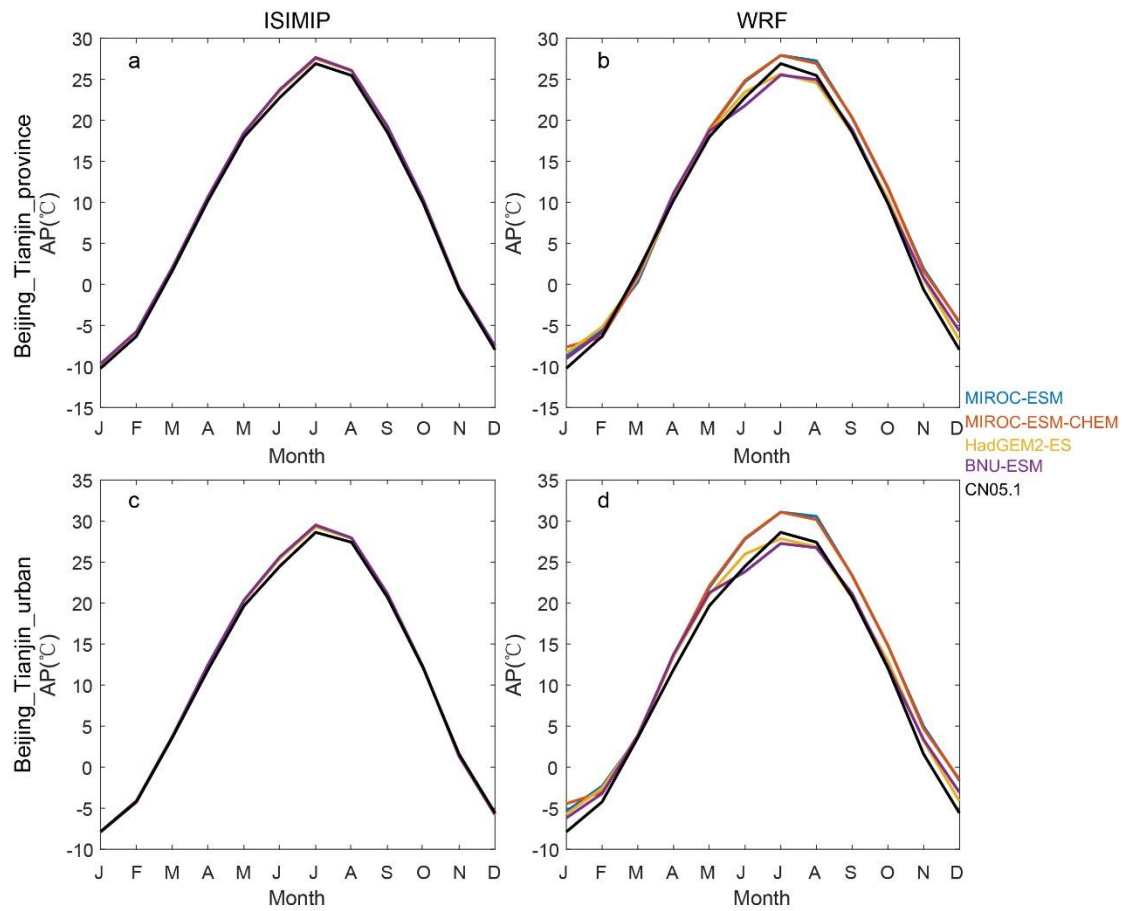


Figure S12. Seasonal cycle of average AP of 4 ESMS under ISIMIP (**a, c**) and WRF (**b, d**) in Beijing-Tianjin province (**a, b**) and Beijing-Tianjin urban areas (**c, d**) during 2008-2017.

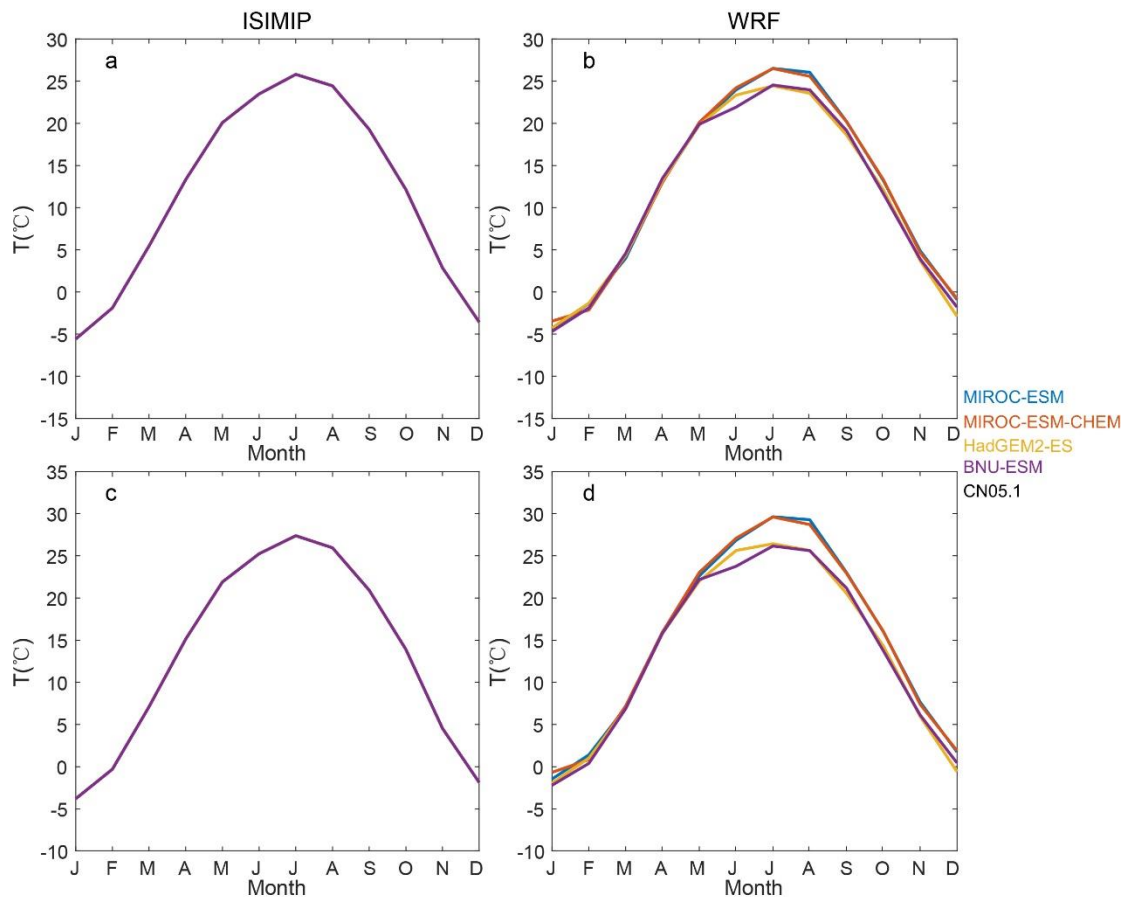


Figure S13. Seasonal cycle of average 2m temperature of 4 ESMs under ISIMIP (**a, c**) and WRF (**b, d**) in Beijing-Tianjin province (**a, b**) and Beijing-Tianjin urban areas (**c, d**) during 2008-2017.

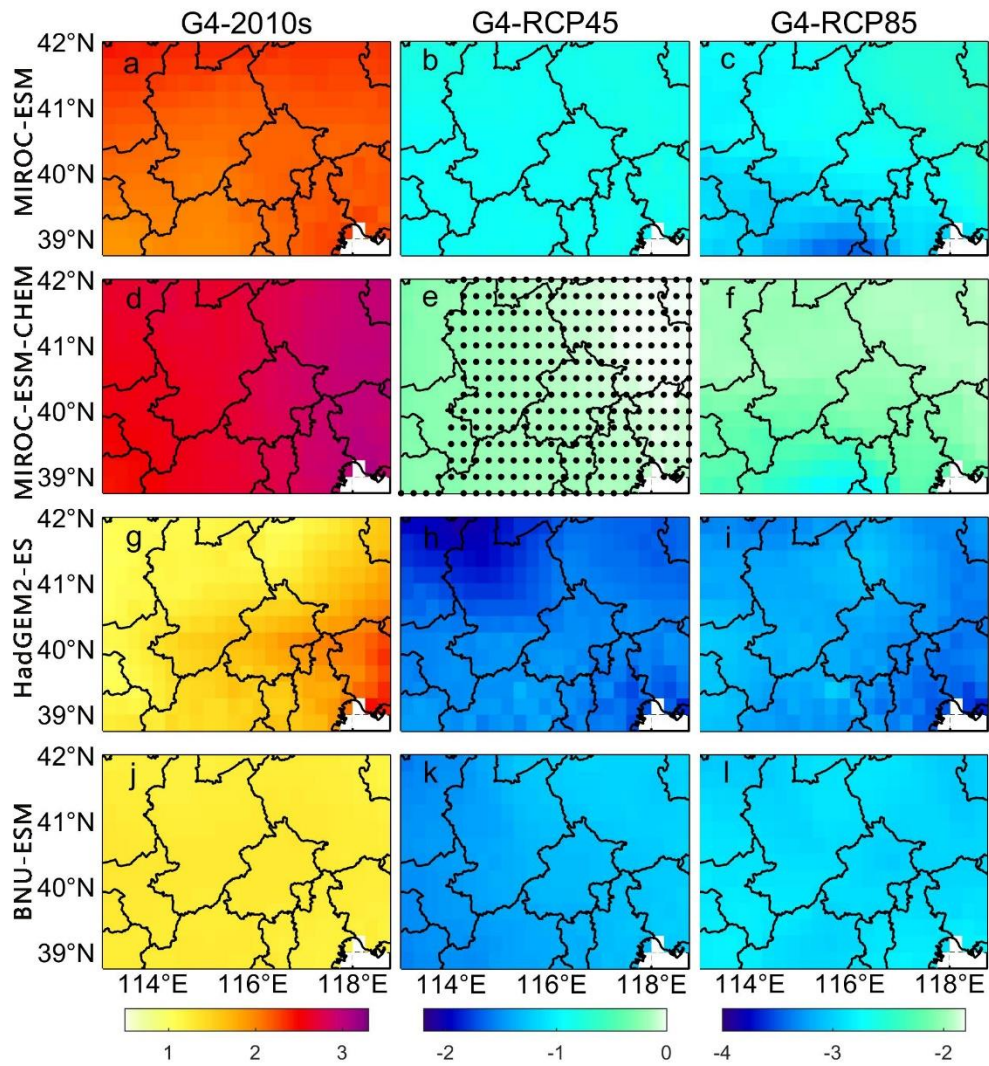


Figure S14. Spatial pattern of apparent temperature difference ($^{\circ}\text{C}$) under different scenarios in 2060-2069: G4-2010s (left column), G4-rcp4.5 (second column) and G4-rcp8.5 (right column) based on ISIMIP method. 2010s means the results simulated during 2008-2017. From top to bottom are MIROC-ESM (a-c), MIROC-ESM-CHEM (d-f), HadGEM2-ES (g-i) and BNU-ESM (j-l), respectively. Stippling indicates grid points where differences or changes are not significant at the 5% level according to the Wilcoxon signed rank test.

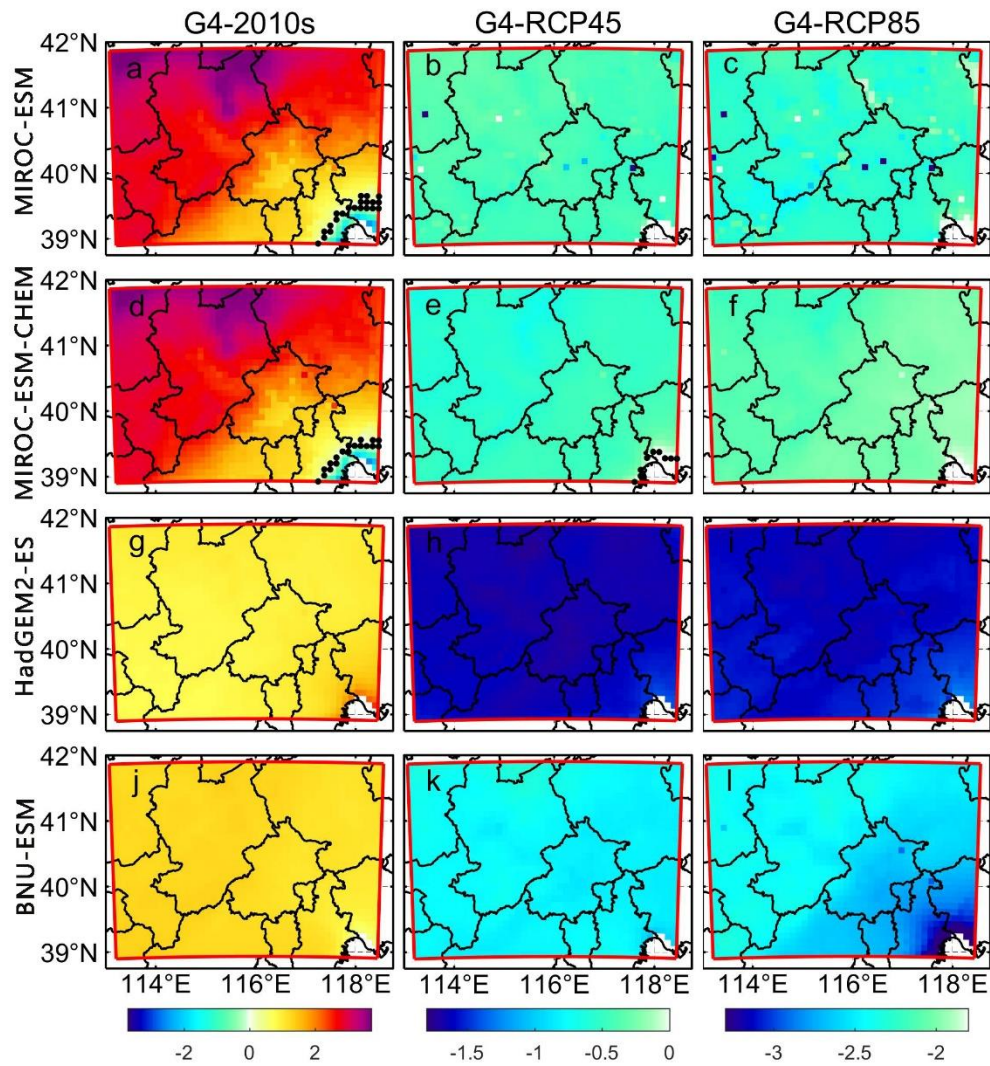


Figure S15. Spatial pattern for apparent temperature difference ($^{\circ}\text{C}$) under different scenarios in 2060-2069: G4-2010s (left column), G4-rcp4.5 (second column) and G4-rcp8.5 (right column) based on WRF_QDM results. 2010s means the results simulated during 2008-2017. From top to bottom are MIROC-ESM (a-c), MIROC-ESM-CHEM (d-f), HadGEM2-ES (g-i) and BNU-ESM (j-l), respectively. Stippling indicates grid points where differences or changes are not significant at the 5% level according to the Wilcoxon signed rank test.

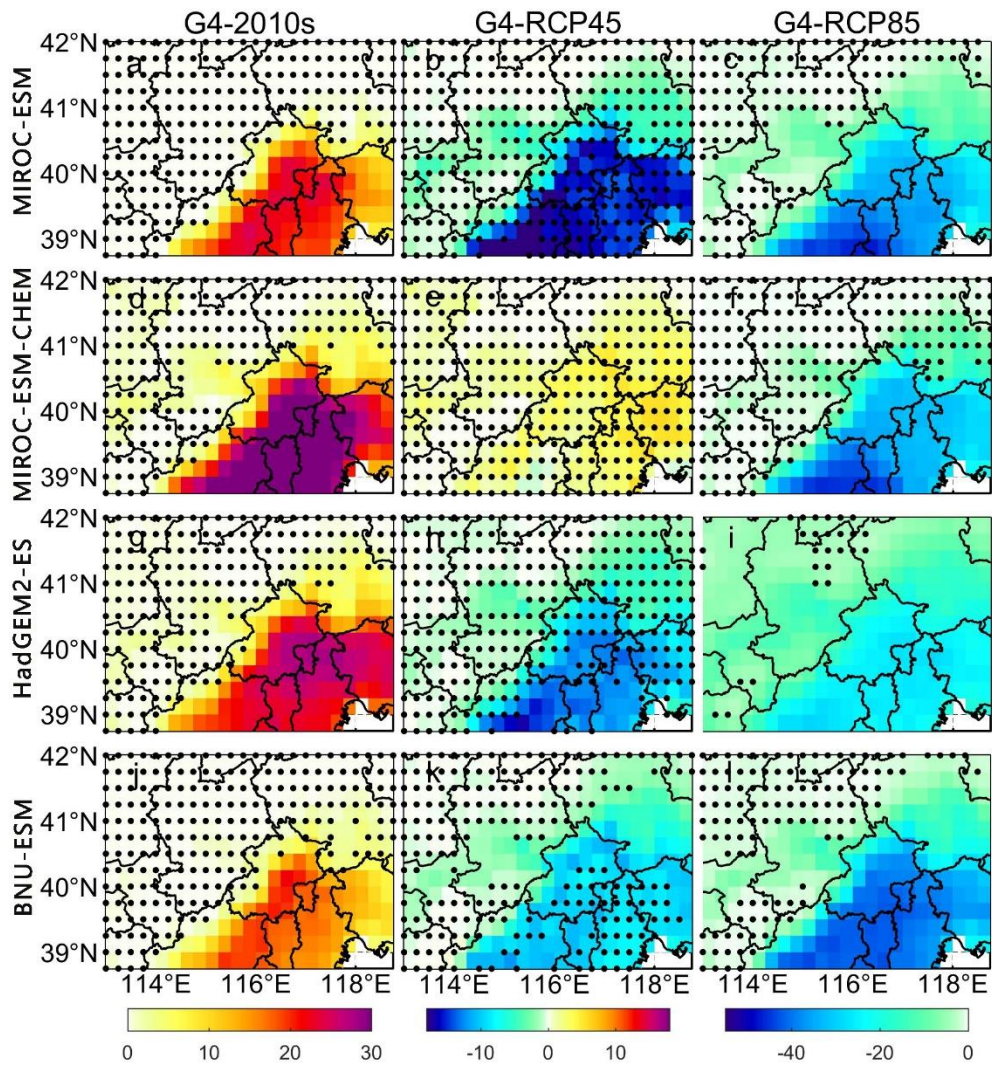


Figure S16. Number of days with AP > 32°C differences under different scenarios over 2060-2069: G4-2010s (left column), G4-rcp4.5 (second column) and G4-rcp8.5 (right column) based on ISIMIP method. 2010s means the results simulated during 2008-2017. From top to bottom are MIROC-ESM (a-c), MIROC-ESM-CHEM (d-f), HadGEM2-ES (g-i) and BNU-ESM (j-l), respectively. Stippling indicates grid points where differences or changes are not significant at the 5% level according to the Wilcoxon signed rank test.

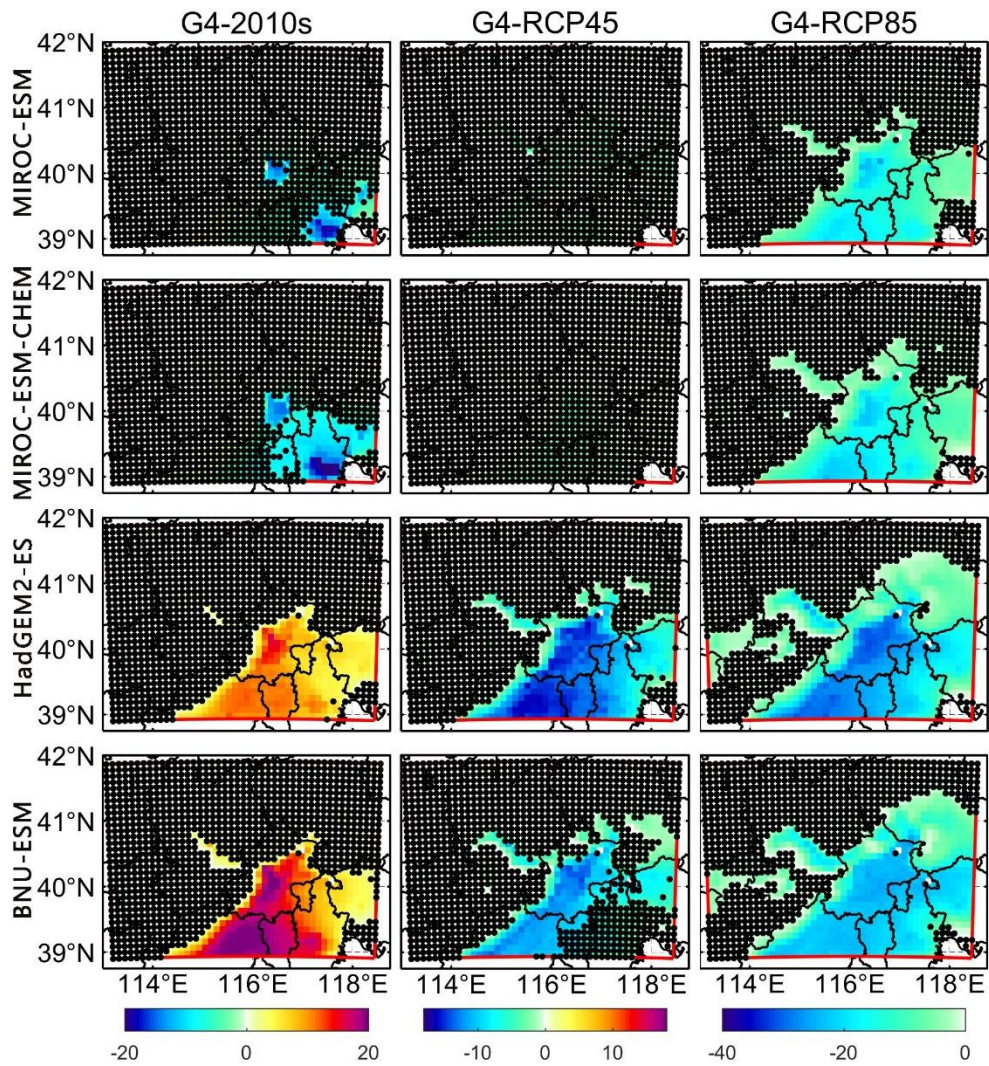


Figure S17. Number of days with AP > 32°C differences under different scenarios over 2060-2069: G4-2010s (left column), G4-rcp4.5 (second column) and G4-rcp8.5 (right column) based on WRF_QDM method. 2010s means the results simulated during 2008-2017. From top to bottom are MIROC-ESM (a-c), MIROC-ESM-CHEM (d-f), HadGEM2-ES (g-i) and BNU-ESM (j-l), respectively. Stippling indicates grid points where differences or changes are not significant at the 5% level according to the Wilcoxon signed rank test.

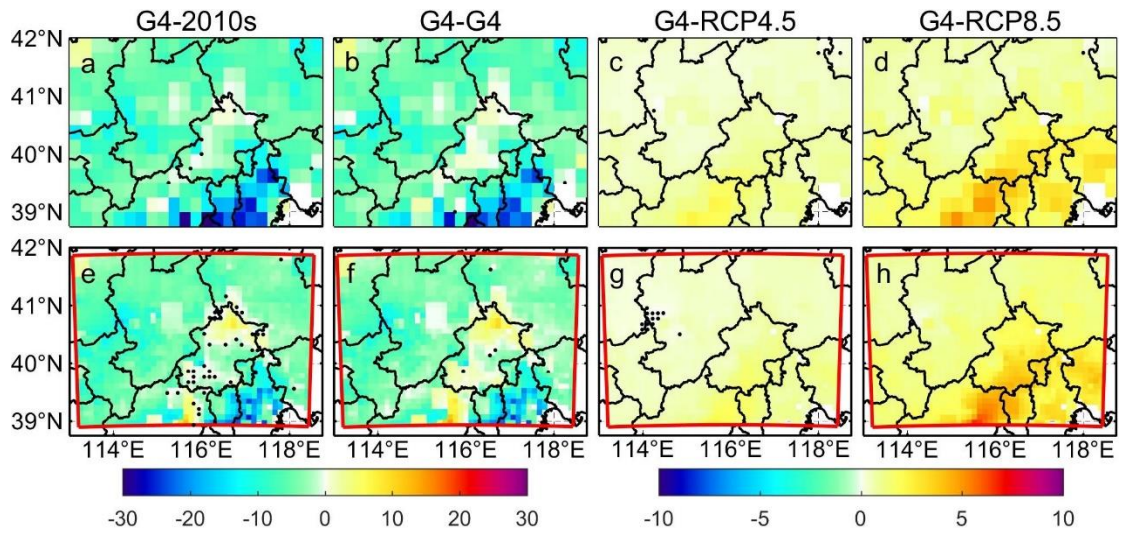


Figure S18. Same as figure 11, but the results of all variables in MLR.

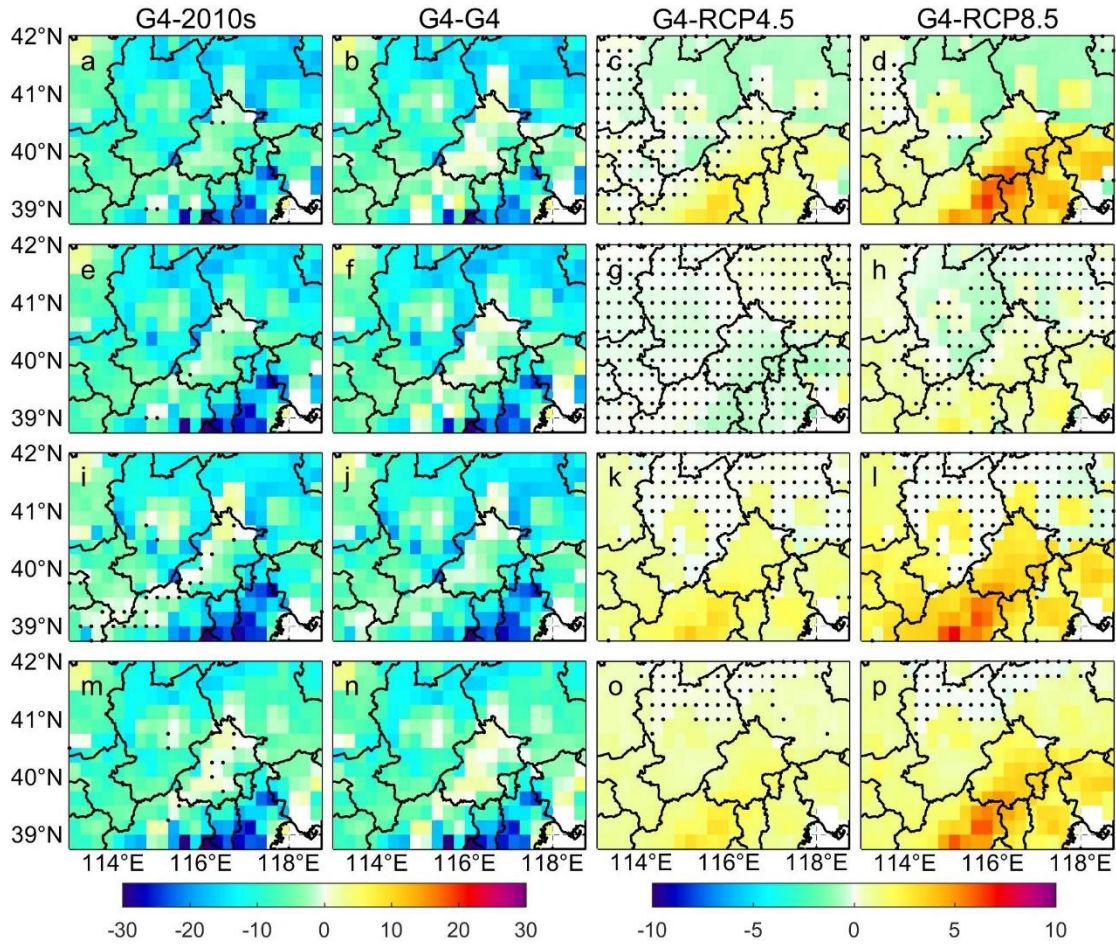


Figure S19. Spatial patterns of $PM_{2.5}$ concentration difference ($\mu g/m^3$) between “mitigation” in the 2060s under G4 and 2010s (**a, e, i, m**), between “mitigation” and “baseline” under G4 (**b, f, j, n**), between G4 and RCP4.5 under “mitigation” scenario (**c, g, k, o**), and between G4 and RCP8.5 under “mitigation” scenario (**d, h, l, p**) based on ISIMIP results. From top to bottom are MIROC-ESM (**a-d**), MIROC-ESM-CHEM (**e-h**), HadGEM2-ES (**i-l**) and BNU-ESM (**m-p**) respectively. Stippling indicates grid points where differences or changes are not significant at the 5% significant level according to the Wilcoxon signed rank test.

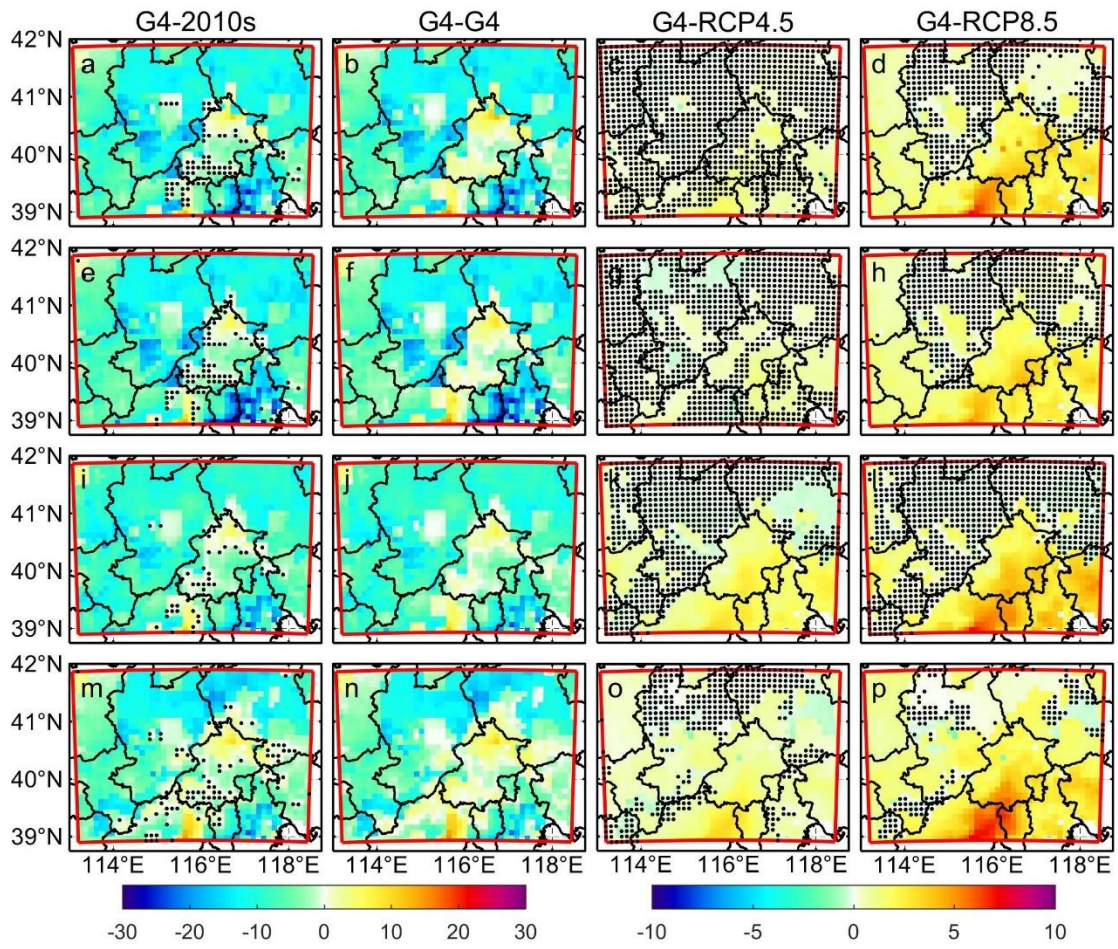


Figure S20. Same as Fig. S19, but by WRF.

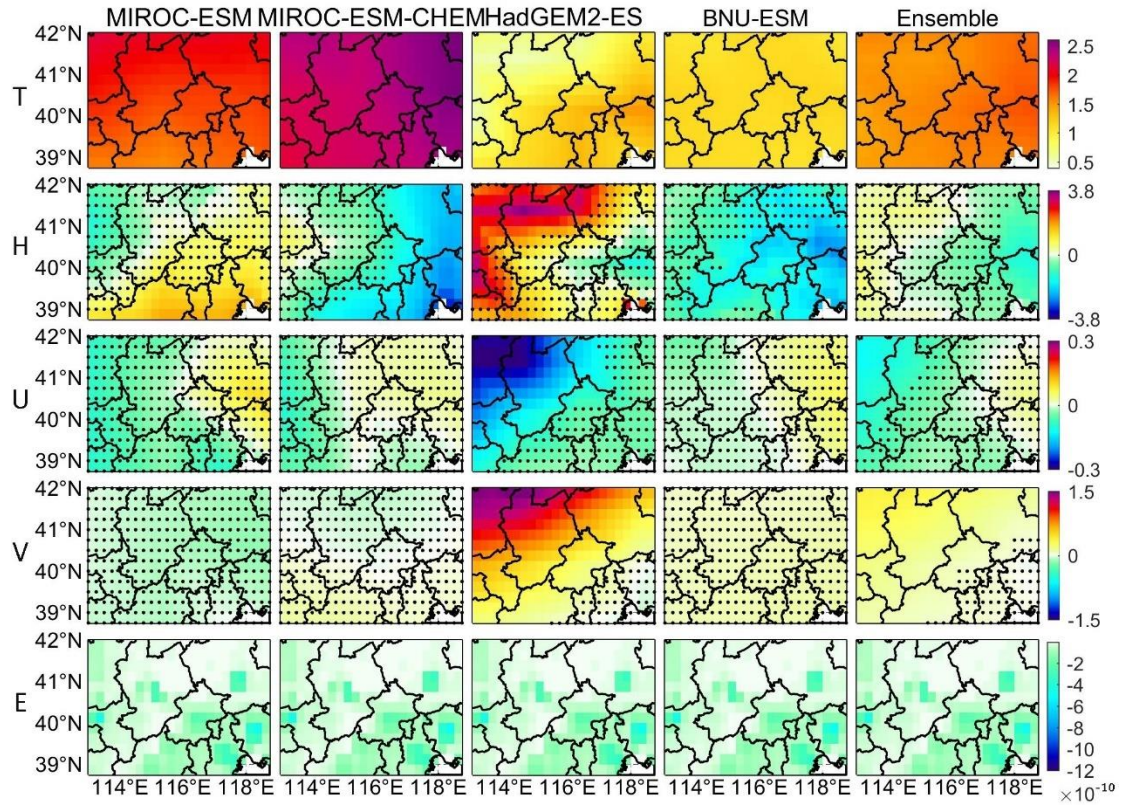


Figure S21. Spatial pattern of changes in temperature (T/°C), humidity (H/%), zonal wind (U/m s⁻¹), meridional wind (V/m s⁻¹) and PM_{2.5} emissions (E/kg m⁻² s⁻¹) under G4 (“mitigation”) in the 2060s relative to 2010s in ISIMIP. Stippling indicates grid points where differences or changes are not significant at the 5% significant level according to the Wilcoxon signed rank test.

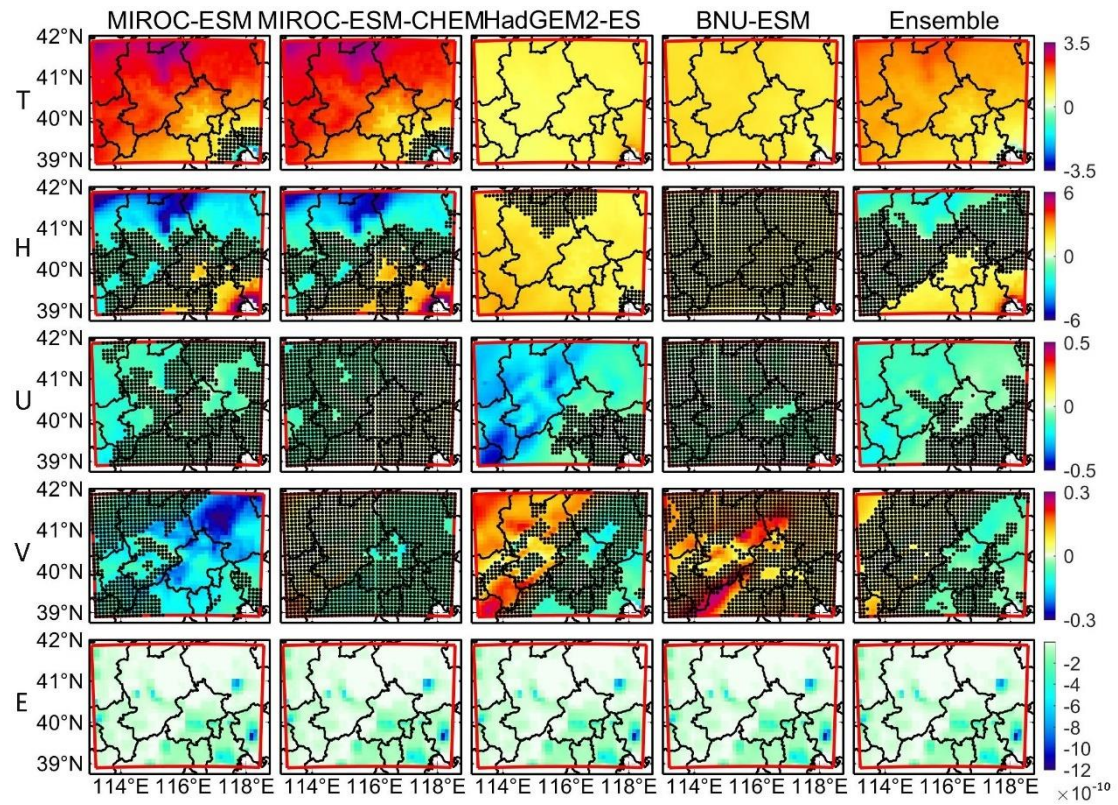


Figure S22. Same as Fig. S21, but by WRF.

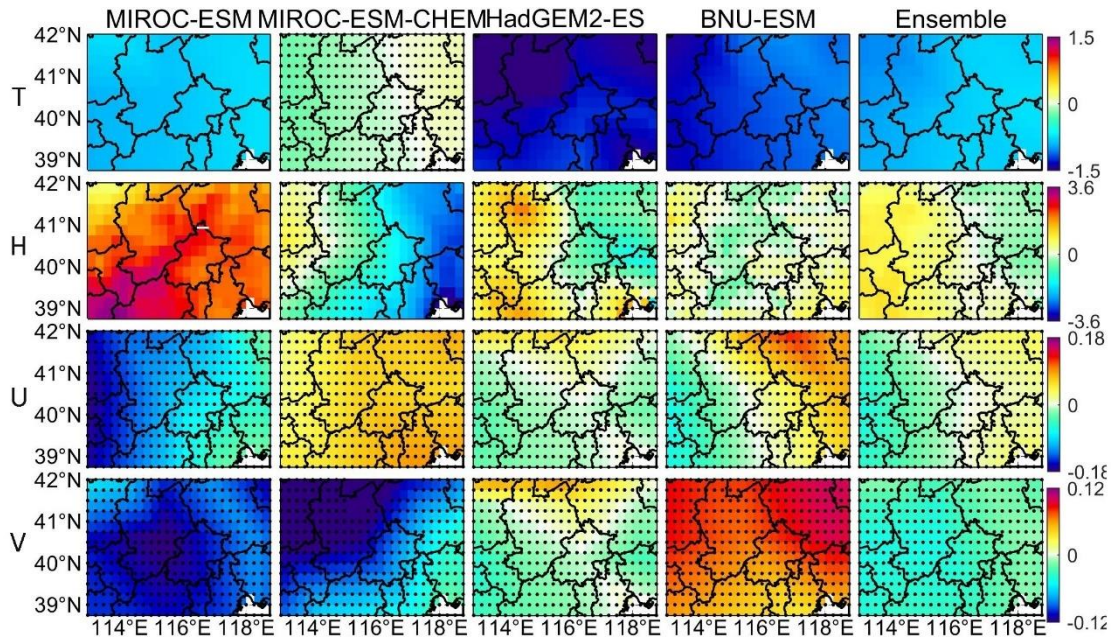


Figure S23. Spatial pattern of changes in temperature ($T/^{\circ}\text{C}$), humidity ($H/\%$), zonal wind ($U/\text{m s}^{-1}$) and meridional wind ($V/\text{m s}^{-1}$) under G4 (“mitigation”) relative to RCP4.5 (“mitigation”) in the 2060s in ISIMIP. Stippling indicates grid points where differences or changes are not significant at the 5% significant level according to the Wilcoxon signed rank test.

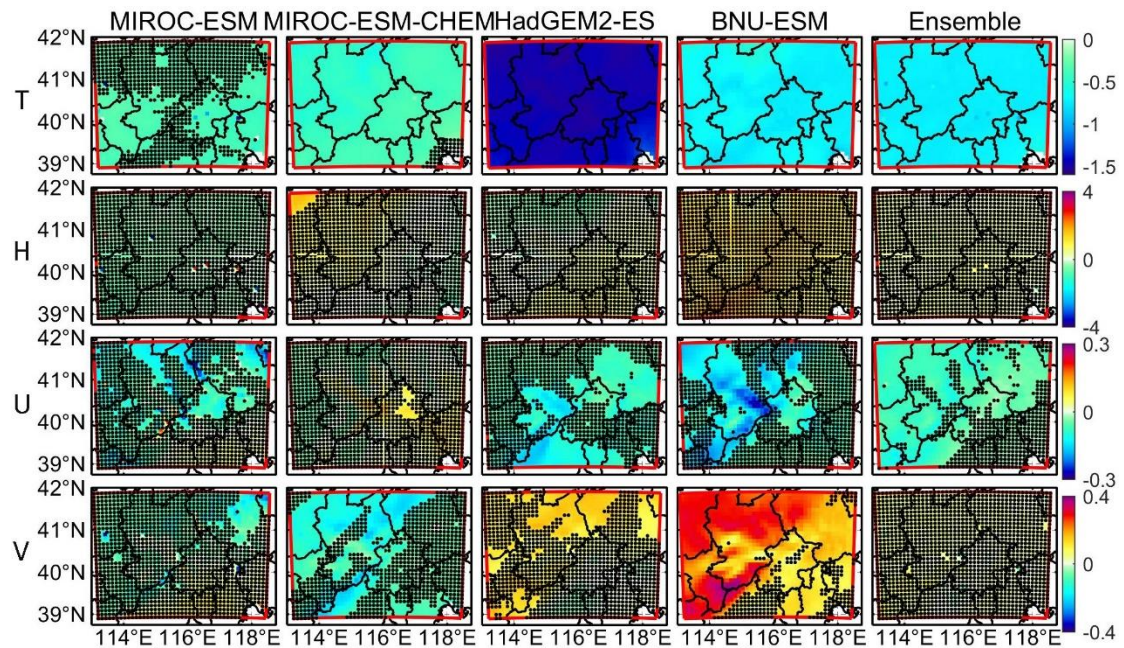


Figure S24. Same as Fig. S23, but for WRF results.

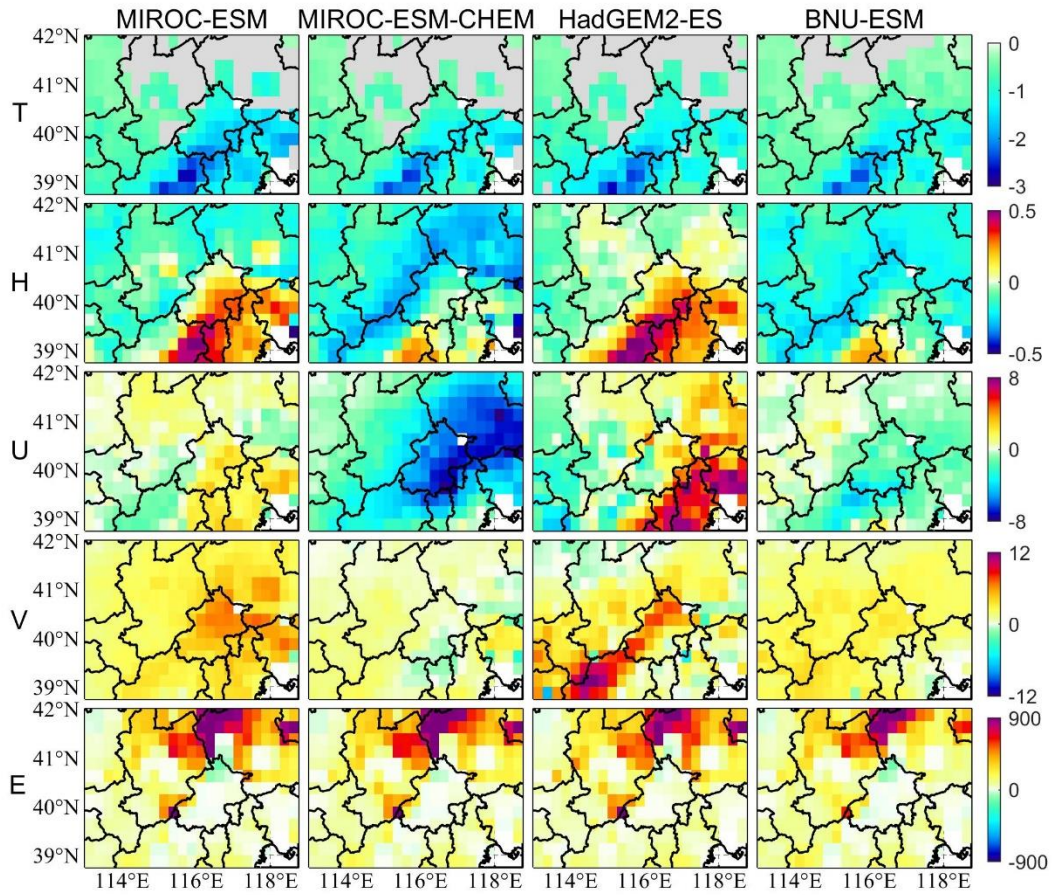


Figure S25. Slope coefficients of MLR of temperature, humidity, u-wind, v-wind and emission for ISIMIP results during training period. The grey areas represent collinearity in the top figures, and we remove the temperature in these areas from our MLR.

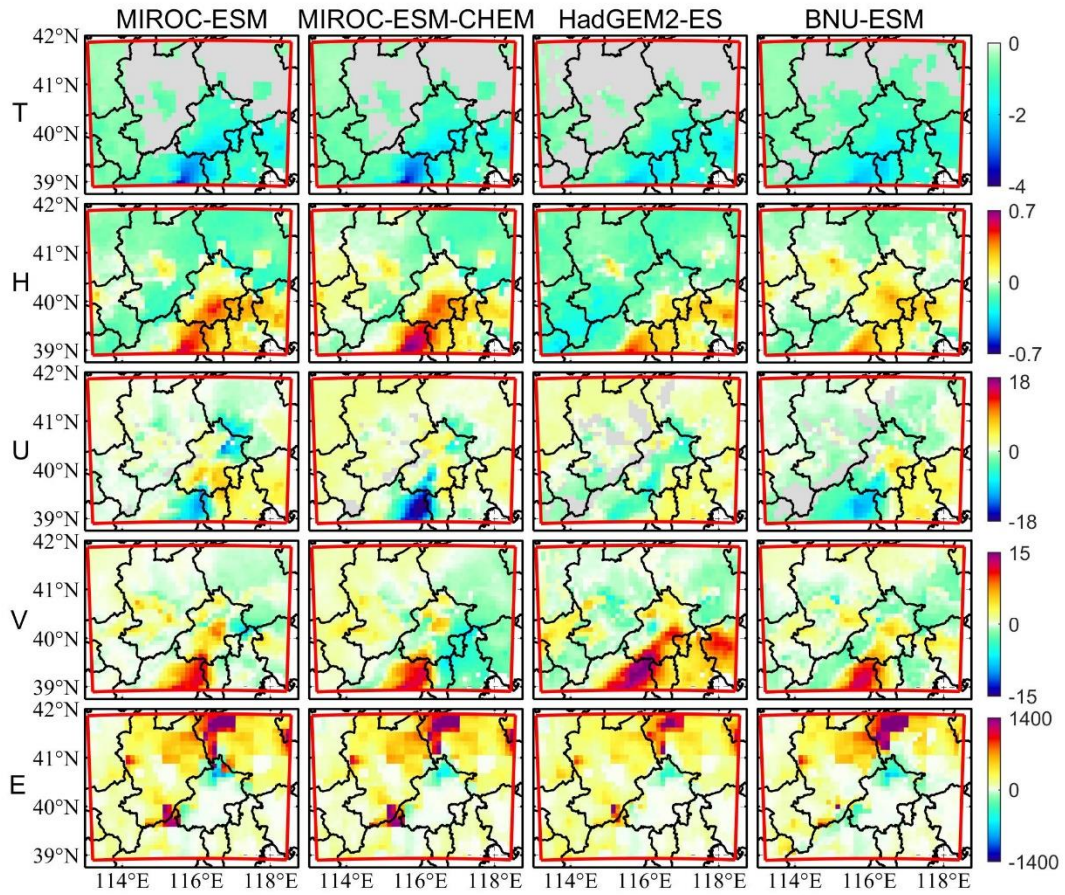


Figure S26. Similar as Fig. S25, but for WRF results. Collinearity exists in first and third rows.

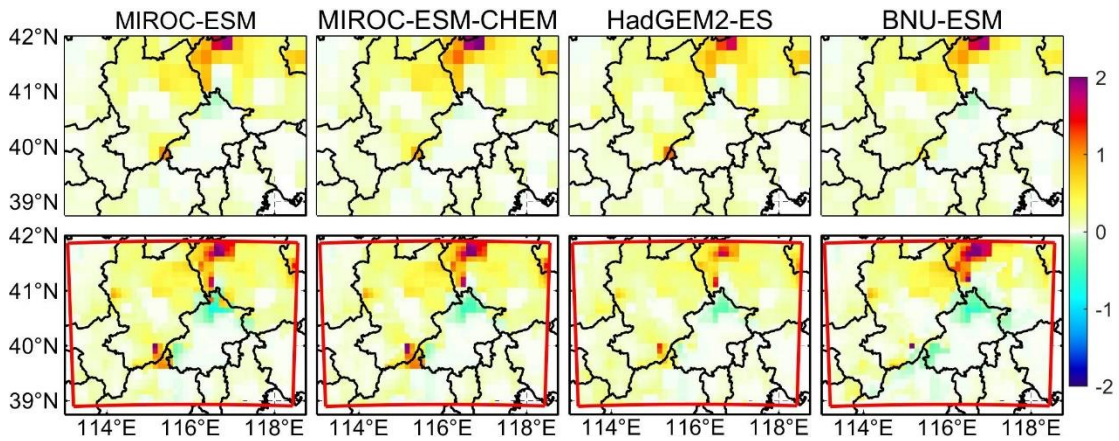


Figure S27. Spatial pattern of changes in $PM_{2.5}$ ($\mu g/m^3$) between G4 with and without considering aerosol deposition due to SAI specified by G4.